


ITC 3/49 Information Technology and Control Vol. 49 / No. 3 / 2020 pp. 299-307 DOI 10.5755/j01.itc.49.3.23998	Synthetic-Aperture Radar Image Despeckling based on Improved Non-Local Means and Non-Subsampled Shearlet Transform	
	Received 2019/08/11	Accepted after revision 2020/08/04
	 <a href="http://dx.doi.org/10.5755/j01.itc.49.3.23998">http://dx.doi.org/10.5755/j01.itc.49.3.23998</a>	

**HOW TO CITE:** Sun, Z., Shi, R., Wei, W. (2020). Synthetic-Aperture Radar Image Despeckling based on Improved Non-Local Means and Non-Subsampled Shearlet Transform. *Information Technology and Control*, 49(3), 299-307. <https://doi.org/10.5755/j01.itc.49.3.23998>

# Synthetic-Aperture Radar Image Despeckling based on Improved Non-Local Means and Non-Subsampled Shearlet Transform

**Zengguo Sun**

Key Laboratory of Modern Teaching Technology, Ministry of Education, Xi'an Shaanxi 710062, China  
School of Computer Science, Shaanxi Normal University, Xi'an 710119, China

**Rui Shi**

School of Computer Science, Shaanxi Normal University, Xi'an 710119, China

**Wei Wei\***

School of Computer Science and Engineering, Xi'an University of Technology, Xi'an 710048, China  
e-mail: [weiwei@xaut.edu.cn](mailto:weiwei@xaut.edu.cn)

\*Corresponding author: [weiwei@xaut.edu.cn](mailto:weiwei@xaut.edu.cn)

When Synthetic-Aperture Radar (SAR) image is transformed into wavelet domain and other transform domains, most of the coefficients of the image are small or zero. This shows that SAR image is sparse. However, speckle can be seen in SAR images. The non-local means (NLM) is a despeckling algorithm, but it cannot overcome the speckle in homogeneous regions and it blurs edge details of the image. In order to solve these problems, an improved NLM is suggested by using  $L_{1/2}$  norm instead of  $L_2$  norm as the measure of similarity. At the same time, the non-subsampled Shearlet transform (NSST) is chosen for effective speckle suppression in edge regions. By combining NSST with improved NLM, a new type of despeckling algorithm is proposed. Experiments demonstrate that the new algorithm leads to satisfying results for SAR images.

**KEYWORDS:** Synthetic-aperture radar image; Despeckling algorithm; NSST; Non-local means.

---

## 1. Introduction

The GF-3 is the first C-band and multi-polarized synthetic-aperture radar (SAR) satellite of 1-metre resolution [36]. It is the only “radar star” in the Gaofen special project. Unlike optical satellites, the biggest advantage of radar satellites is that they can work all-day, all-weather. The GF-3 satellite observes targets by launching microwaves. Ground targets can be imaged at any time, whether day or night, sunny or rainy. This feature is especially suitable for disaster prevention and mitigation [24], oil spill detection [3], and semantic segmentation of remote sensing images [4]. However, speckle appearing in SAR images impedes comprehension of images themselves. Therefore, despeckling is still difficult in SAR images processing [23]. When SAR image is transformed into wavelet domain and other transform domains, most of the transformed coefficients of the image are small or zero, i.e., the SAR image is sparse. Especially for the GF-3 images, positions and geometric structures such as point targets, textures and edges are so clear, which indicates that GF-3 images have clear sparsity. The use of this sparsity is helpful for construction of efficient despeckling methods. However, traditional Lee filter [16, 35], Kuan filter [14, 25] and Gamma MAP filter [26], which ignore the use of such sparsity, cannot achieve a promising speckle smoothing for SAR images.

The non-local means (NLM) algorithm is a filtering algorithm that has emerged in recent years [37]. The core idea is that the value of one pixel has a correlation with the value of the other pixels in each image. By selecting a fixed-size image block and then choosing the other image block that is similar with the fixed-size image block in the entire image, speckle can be suppressed by the value of the weight according to the similarity. This method cannot efficiently reduce speckles in homogeneous region and it obscures edge details of the image. The main reason is that the traditional NLM uses the  $L_2$  norm as the measure of the similarity. In [31], the  $L_{1/2}$  regularization leads to much more clear sparse solution in comparison with the  $L_2$ , which means that the  $L_{1/2}$  norm performs better sparsity than the  $L_2$  norm. So the traditional NLM is not applicable for the SAR images with strong sparsity. In recent years, the NLM principle is widely used in image processing. In [6], a new method of patch

similarity was defined under the non-Gaussian noise. In [7], a new method named NL-SAR was proposed to process the speckle. It should be noted that these two methods are all the spatial-domain filtering. The proposed method is built on the domain of Shearlet transform. Shearlet has optimal sparsity and can handle high-resolution SAR images with sparse features.

Here despeckling algorithm is constructed by using good sparsity of SAR images. Therefore, an improved NLM is suggested that uses  $L_{1/2}$  norm instead of  $L_2$  norm as the measure of the similarity. The  $L_{1/2}$  norm is demonstrated to be much sparser compared to the  $L_2$  norm [22], so the improved NLM can lead to better despeckling results, i.e., smoothing speckle and preserving edges. It should be noted that the improved NLM cannot smooth speckle sufficiently in edge regions. This drawback can be eliminated by Shearlet.

Multiscale geometric analysis (MGA) has been extensively used in image processing [15, 19]. Shearlet is MGA method that has best sparse representation, so it can be effectively applied to SAR images with obvious sparse features. Therefore, to better suppress the speckle in edge regions in SAR images, Shearlet is used for the construction of the new despeckling algorithm. At the same time, the non-subsampled Shearlet transform (NSST) is chosen for replacing the traditional one because traditional Shearlet transform will cause the phenomenon of spectrum aliasing. In [12], a new despeckling method was proposed based on the adaptive threshold and NSST, which is an application of the optimal sparse Shearlet. However, our proposed method combines the improved NLM with NSST, so it can sufficiently reflect the sparsity of SAR images. The proposed method reduces speckle in homogeneous areas, effectively preserves edge information, and better smoothes speckle in edge areas, leading to a satisfying performance for SAR images.

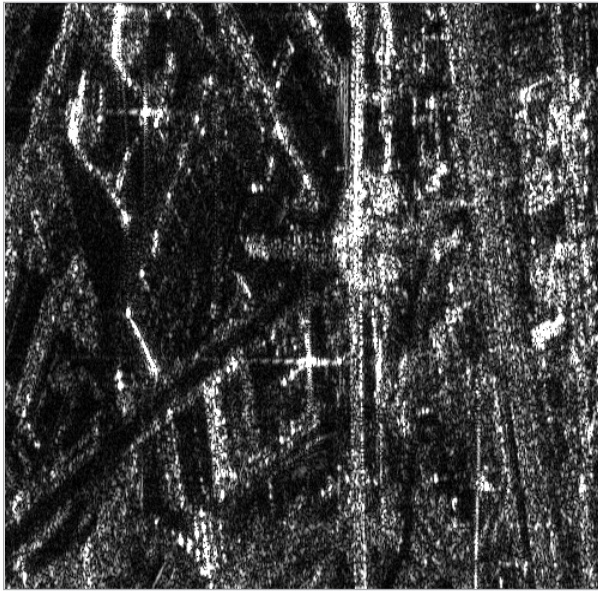
---

## 2. Brief Introduction of SAR Images

GF-3 has the richest imaging modes at present. Moreover, it can transmit and receive horizontal waves and vertical waves at the same time [18]. Figure 1 is a scene of SAR image of Nanjing. We can see that SAR

**Figure 1**

A scene of SAR image of city from GF-3



images have obvious position information and geometric structures. Table 1 is the corresponding imaging parameters. From the image it can be seen that edges, points, and textures are so clear, which denotes that SAR images have good sparsity. However, speckle appears in SAR images, which burdens the interpretation of images. Thus we need to remove speckle from SAR images.

**Table 1**

Imaging parameters of Figure 1

Ground receiving station	Imaging mode	Resolution	Imaging position	Polarization
MDJ	SL	0.5m	E114.4 N30.5	vv

### 3. NLM and Its Improvement

Different from the traditional Lee, Kuan and Gamma MAP filters, the NLM filter adopts image redundancy and fully considers similarity structure information of the image. By selecting a fixed-size image block and then choosing another image block that is similar with the fixed-size image block in the entire image,

speckle can be suppressed by the value of the weight according to the similarity [34].

Denoting  $v = \{v(x)|x \in I\}$  ( $I$  represents image domain) as a scene of a SAR image, the NLM is defined by

$$NL[v](i) = \sum_{j \in I} w(i, j)v(j), \tag{1}$$

where  $NL[v](i)$  denotes despeckling result,  $w(i, j)$  ( $0 \leq w(i, j) \leq 1, \sum w(i, j) = 1$ ) is weight value, indicating the impact of  $j$  on  $i$ . The similarity is higher if the weight value is higher. Here,

$$w(i, j) = \frac{1}{C(i)} e^{-\frac{d(i, j)}{h^2}}, \tag{2}$$

$$C(i) = \sum_j e^{-\frac{d(i, j)}{h^2}}, \tag{3}$$

$$d(i, j) = \|v(i) - v(j)\|_{2, \alpha}^2, \tag{4}$$

where  $C(i)$  represents normalized coefficient,  $v(i)$  is image block centred on  $i$ ,  $v(j)$  is image block centred on  $j$ ,  $\|\cdot\|_2$  is the  $L_2$  norm,  $h$  denotes smoothing factor,  $\alpha$  is standard deviation of Gauss kernel, and  $d$  denotes the Gaussian weighted Euclidean distance that represents the degree of similarity among pixels.

When SAR image is transformed into wavelet domain and other transform domains, it is found that most of the coefficients of the image are small or zero. This means that the SAR image is sparse. Although SAR images show obvious sparsity, but the traditional NLM uses the  $L_2$  norm as the measure of similarity. It should be noted that the  $L_2$  norm does not have good sparsity. Thus, the traditional NLM is not applicable for despeckling of SAR images with obvious sparsity. In recent years, the  $L_{1/2}$  norm is proposed with promising performance, especially the good sparsity, and it is extensively used in the domain of signal and image processing [1, 5, 11, 13, 32]. Motivated by this, we use  $L_{1/2}$  norm instead of  $L_2$  norm as the measure of similarity to obtain the improved NLM.

The common norms include  $L_0$  norm,  $L_1$  norm,  $L_2$  norm, and  $L_\infty$  norm. For  $X = (x_1, x_2, \dots, x_n)$ , the above norm is defined as follows:  $L_0$  norm is the number

of the non-zero elements in the  $X$ .  $L_1$  norm is defined by  $L_1 = \left( \sum |x_i| \right)$ .  $L_2$  norm is the square root of the sum of the squares of the elements in the  $X$ , i.e.,  $L_2 = \left( \sum_i |x_i|^2 \right)^{1/2}$ . The so-called Euclidean distance is a kind of  $L_2$  norm.  $L_\infty$  norm is defined by  $L_\infty = \max(|x_i|)$ . In addition to the above common norms, one can also define the  $L_p$  norm ( $0 < p < 1$ ).

$$L_p = \left( \sum_i |x_i|^p \right)^{1/p}, \quad (0 < p < 1). \tag{5}$$

In each of the above norms, the  $L_0$  norm has the optimal sparsity, but the  $L_0$  norm does not have the specific mathematical theory. Compared with other norms (except for the  $L_0$  norm), the  $L_p$  ( $0 < p < 1$ ) norm has the better sparsity, and the sparsity is stronger if the  $p$  is smaller. Particularly, the  $L_{1/2}$  norm has the complete mathematical theory and its sparsity is very close to the  $L_p$  norm when  $0 < p < 1$ . So the  $L_{1/2}$  norm is adopted to measure the similarity instead of the  $L_2$  norm, leading to the improved NLM with

$$d(i, j) = \|v_i - v_j\|_{1/2, \alpha}^2. \tag{6}$$

### 4. Proposed Despeckling Algorithm Based on Improved NLM and NSST

Compared to traditional NLM, the improved NLM can effectively smooth speckle in homogeneous areas and well preserve edge information. However, this method cannot sufficiently smooth speckle in edge regions. Recalling the obvious sparsity of SAR images, the most sparse Shearlet is applied, and then the improved NLM is adopted in Shearlet transform domain to obtain optimum performance.

#### 4.1. Basic Concept of Shearlet

The definition of Shearlet is introduced in [9], including its composition and local characteristics.

Particularly, Shearlet has the optimum sparsity, i.e., it holds

$$\|f - f_N^s\|_2^2 \leq CN^{-2} (\log N)^3. \tag{6}$$

where  $f$  denotes a specific function, and  $f_N^s$  is its approximation with maximum Shearlet coefficient of count  $N$ . Obviously, Shearlet is the most sparse tool, describing images with edges in all scales and directions the most accurately [17]. As the optimal sparse tool, the Shearlet can subdue speckle sufficiently in the homogeneous areas, effectively preserve edge information, and effectively smooth speckle in edge areas for SAR images with obvious sparsity.

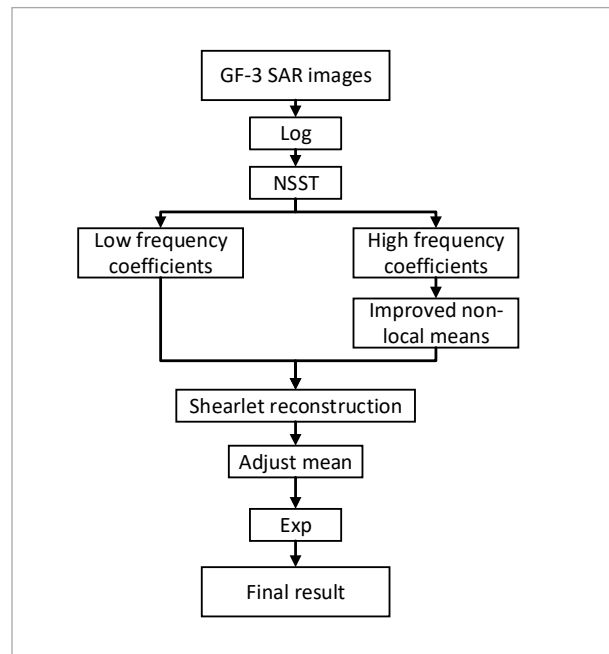
#### 4.2. Proposed Despeckling Method

Laplacian decomposition filter banks are used in the traditional Shearlet transform, resulting in aliasing if downsampling is used.

NSST is applied to construct the despeckling algorithm. Since the mean in log is biased, specific correcting method should be adopted. In [29], mean adjustment was applied between Shearlet reconstruction and “exp” operation, subtracting the mean value of log-transformed speckle from the result of Shearlet reconstruction. The flowchart of proposed algorithm is shown in Figure 2 and the specific steps about the suggested algorithm are explained as follows:

**Step 1:** Log-transformed is used for SAR images.

Figure 2  
Flowchart of proposed despeckling algorithm



**Step 2:** NSST is performed on the result of above step to obtain the Shearlet coefficients, and the improved NLM is used for high frequency coefficients.

**Step 3:** Shearlet reconstruction is performed.

**Step 4:** Resulting image is obtained by performing the mean adjust and the exponential operation successively.

In a word, above method is presented for the GF-3 images. The motivation is explained detailedly here. The GF-3 images own obvious sparsity, according to the analysis of the wavelet-transformed coefficients of images described in Section 1 and the characteristics of clear position information and geometric structures in images explained in Section 2. Consideration of such sparsity is indispensable for construction of efficient despeckling algorithms for GF-3 images. The NLM is used in this paper. Since the  $L_{1/2}$  norm performs better sparsity than the traditional  $L_2$  norm, the improved NLM is obtained by using the  $L_{1/2}$  norm instead of  $L_2$  norm as the measure of similarity to reflect sparsity of GF-3 images. Additionally, as the optimal sparse tool, Shearlet is applied firstly for images and then the improved NLM is adopted in Shearlet transform domain in order to further reflect the sparsity of the GF-3 images, leading to the presented despeckling algorithm. Therefore, combined use of the  $L_{1/2}$  norm and Shearlet is so appropriate for despeckling of GF-3 images with clear sparsity.

## 5. Experimental Results

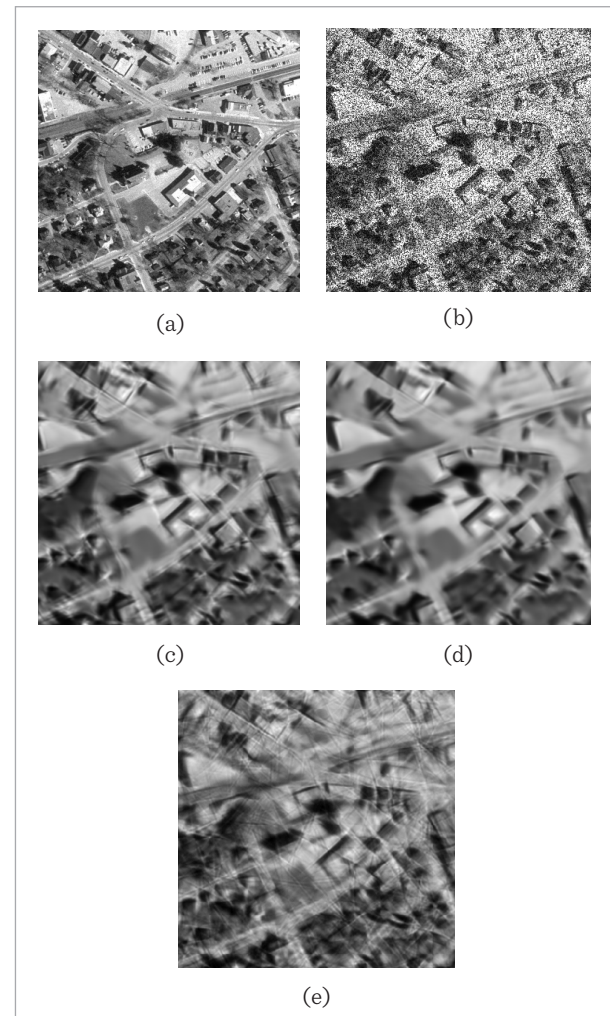
The purpose of our experiments is not to explain details of each method, but to explain the filtering principles as follows [8, 10]:

- 1 The NLM is proposed in [2] according to a non-local averaging of all image pixels. It uses  $L_2$  norm as similarity of the pixels.
- 2 Compared to traditional NLM, the improved NLM uses a better way to measure the similarity of the pixels, and it chooses the  $L_{1/2}$  norm as the similarity of the pixels.
- 3 By combining improved NLM with NSST, the proposed method is constructed. The proposed method uses Shearlet and  $L_{1/2}$  norm with better sparsity, leading to a satisfying performance for SAR images.

We started by an aerial image which was selected because of the similar content to true SAR images. We adopted the level of simulated speckle noise in intensity format equivalent to  $\sigma^2=0.2$  ( $\sigma^2$  is the variance of speckle). The despeckling results are shown in Figure 3. Obviously, the traditional NLM cannot suppress the speckle sufficiently because it does not consider the sparsity of SAR images, and the edges and fine details are somewhat blurred. By using the  $L_{1/2}$  norm which has better sparsity than the  $L_2$  norm as the measure of similarity, the improved NLM effectively smoothes speckle in homogeneous areas and well preserves

**Figure 3**

Despeckling experiments on the aerial image. (a) real image, (b) image corrupted by simulated speckle noise ( $\sigma^2=0.2$ ), (c) NLM, (d) improved NLM, and (e) proposed algorithm



edge information. The proposed method combines optimal sparse Shearlet with the improved NLM. It sufficiently smoothes speckle in homogeneous areas as well as in edge areas, and effectively keeps edges and fine details.

Two scenes of SAR images in Figure 4 are chosen for despeckling experiments, and the corresponding imaging parameters are provided in Table 2.

**Figure 4**

Two scenes of SAR images: (a) Image one, (b) Image two

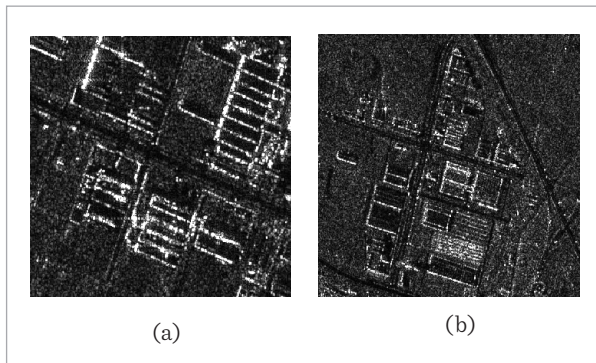


**Table 2**

Imaging parameters of SAR images

No	Imaging model	Resolution	Imaging position	Polarization
Figure 4(a)	FSI	5m	E113.4 N34.7	HH
Figure 4(b)	FSI	5m	E113.2 N34.5	HH

The despeckling experiments on Figure 4(a) are provided in Figure 5, and corresponding evaluating measures are given in Table 3. Equivalent Number of Looks (ENL) is defined by ratio of mean square to variance in a homogeneous region [20]. Bigger ENL means higher speckle suppression of algorithm. Difference of Coefficient of Variations (DCV) is used to reflect the ability of edge preservation [28]. Smaller DCV means better edge preservation. It can be seen that traditional NLM does not consider the sparsity of SAR images, so the speckle is not suppressed sufficiently, and the edges and fine details are somewhat blurred. By using the  $L_{1/2}$  norm as the measure of similarity, the improved NLM not only effectively reduc-

es speckle in the homogeneous regions, but also well preserves the edges and fine details. Therefore, the improved NLM produces greater ENL and smaller DCV in comparison with the traditional NLM. The proposed algorithm combines the optimal sparse Shearlet with the improved NLM, so it sufficiently subdues speckle in homogeneous areas and in edge areas, and efficiently preserves edge information.

**Figure 5**

Despeckling of the SAR image in Figure 4(a). (a) original image, (b) NLM, (c) improved NLM, and (d) proposed algorithm

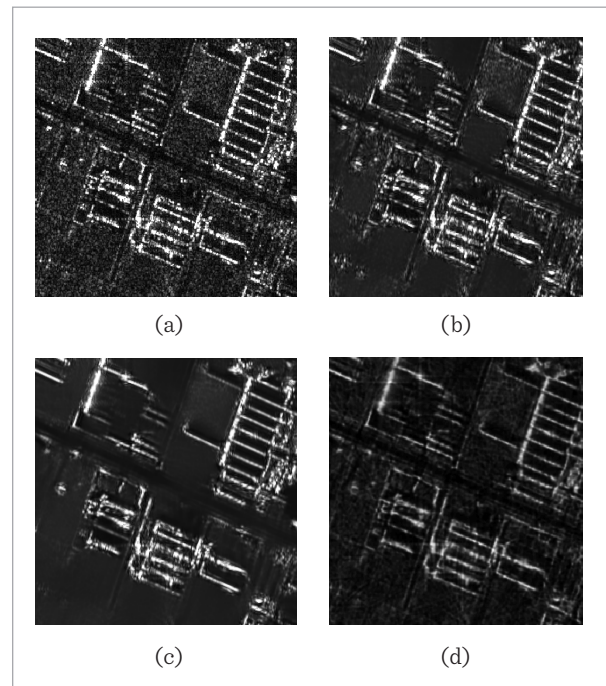


**Table 3**

Quantitative measures of various despeckling methods in Figure 5

	Non-local means	Improved non-local means	Proposed method
ENL	1.12	1.24	1.42
DCV	0.10	0.08	0.06

The other despeckling experiment on Figure 4(b) is shown in Figure 6. The corresponding speckle pattern in Figure 7 is used to qualitatively evaluate despeck-

ling algorithms [27]. The ideal speckle pattern only contains speckle, not including any edge information. It can be seen that the traditional NLM blurs edges seriously, and its speckle pattern contains plenty of edge information. Compared to the traditional NLM, the

**Figure 6**

Despeckling of the SAR image in Figure 4(b). (a) original image, (b) NLM, (c) improved NLM, and (d) proposed algorithm

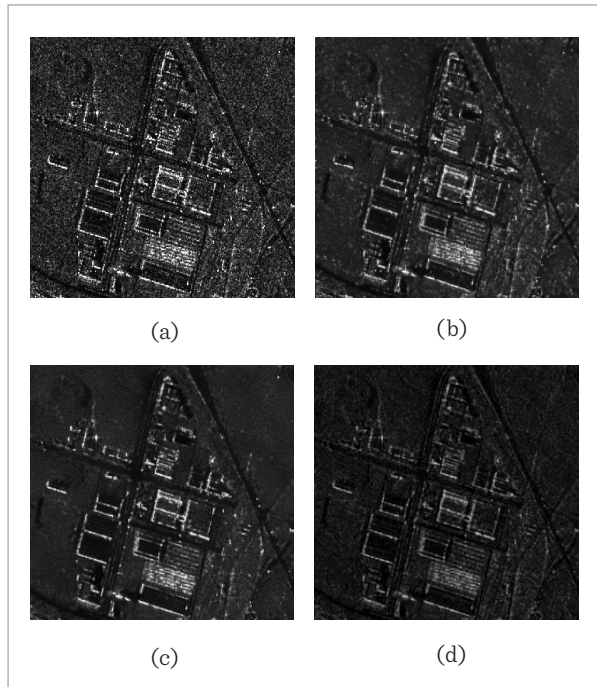
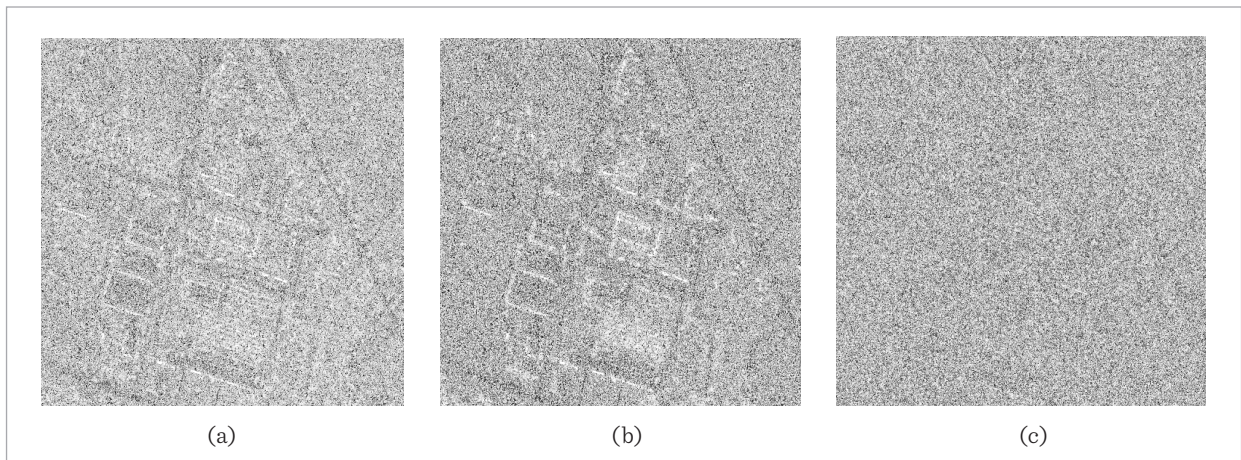


**Figure 7**

Speckle pattern corresponding to Figure 6. (a) NLM, (b) improved NLM, and (c) proposed method



improved NLM preserves edge information better, but it cannot sufficiently suppress speckle in edge regions. Therefore, many edge regions in corresponding speckle pattern are blank, not covered by speckle. The proposed despeckling algorithm using improved NLM and NSST together effectively reduces speckle in homogeneous and edge areas, and efficiently keeps edge information, producing much more ideal speckle pattern [21, 30, 33].

## 6. Conclusion

SAR images own obvious sparsity, but appearance of speckle greatly hinders the interpretation of images. A promising despeckling method must be constructed based on the sparsity of SAR images. The traditional NLM does not reflect the sparsity of SAR images, because it uses  $L_2$  norm as the measure of similarity. The improved NLM is thus proposed which uses  $L_{1/2}$  norm instead of  $L_2$  norm as the measure of similarity. It should be noted that the  $L_{1/2}$  norm has better sparsity than the  $L_2$  norm. Compared to the traditional NLM, the improved NLM achieves better performance, but it cannot sufficiently smooth speckle in edge regions. As the optimal sparse representation tool, Shearlet is adopted in the construction of a despeckling filter. Combined the improved NLM based on  $L_{1/2}$  norm with NSST, a new despeckling method is proposed, which fully reflects the sparsity of SAR images. Despeckling experiments

on simulated and real SAR images demonstrate that, the proposed method can sufficiently overcome speckle in homogeneous and edge areas, and effectively keep edge information. Therefore, the proposed algorithm using improved NLM and NSST together is applicable for the despeckling of SAR images.

## Acknowledgments

This work is supported by the National key R&D Program of China (Nos. 2016YFC0501601, 2018YFB0203901), the National Natural Science Foundation of China

(Nos. 41771118, 61102163), the Fundamental Research Funds for the Central Universities (Nos. GK201903085, 2572018BF04, GK201802004.), and the Key Research and Development Program of Shaanxi Province (No. 2018ZDXM-GY-036). This work is also supported by Key Laboratory of Land Satellite Remote Sensing Application Center, Ministry of Natural Resources of the People's Republic of China (No. KLSMNR-202004). The authors would like to thank the China Centre for Resources Satellite Data and Application for providing the GF-3 SAR images.

## References

1. Bruckstein, A. M., Donoho, D. L., Elad, M. From Sparse Solutions of Systems of Equations to Sparse Modeling of Signals and Images. *Siam Review*, 2009, 51(1), 34-81. <https://doi.org/10.1137/060657704>
2. Buades, A., Coll, B., Morel, J. M. Non-Local Means Denoising. *Image Processing on Line*, 2011, 1, 208-212. [https://doi.org/10.5201/ipol.2011.bcm\\_nlm](https://doi.org/10.5201/ipol.2011.bcm_nlm)
3. Capizzi, G., Lo Sciuto, G., Woźniak, M., Damaševičius, R. A Clustering Based System for Automated Oil Spill Detection by Satellite Remote Sensing. *International Conference on Artificial Intelligence and Soft Computing*, Springer, Cham, 2016, 613-623. [https://doi.org/10.1007/978-3-319-39384-1\\_54](https://doi.org/10.1007/978-3-319-39384-1_54)
4. Chen, G., Li, C., Wei, W., Jing, W., Woźniak, M., Blažauskas, T., Damaševičius, R. Fully Convolutional Neural Network with Augmented Atrous Spatial Pyramid Pool and Fully Connected Fusion Path for High Resolution Remote Sensing Image Segmentation. *Applied Sciences*, 2019, 9(9), 1816. <https://doi.org/10.3390/app9091816>
5. Damasevicius, R., Maskeliunas, R., Wozniak, M., Polap, D., Sidekerskiene, T., Gabryel, M. Detection of Saliency Map as Image Feature Outliers Using Random Projections Based Method. In *2017 13th International Computer Engineering Conference (ICENCO)*, IEEE, 2017, 85-90. <https://doi.org/10.1109/ICENCO.2017.8289768>
6. Deledalle, C. A., Denis, L., Tupin, F. How to Compare Noisy Patches? Patch Similarity Beyond Gaussian Noise. *International Journal of Computer Vision*, 2012, 99(1), 86-102. <https://doi.org/10.1007/s11263-012-0519-6>
7. Deledalle, C. A., Denis, L., Tupin, F., Reigber, A., Jäger, M. NL-SAR: A Unified Nonlocal Framework for Resolution-preserving (Pol)(In)SAR Denoising. *IEEE Transactions on Geoscience and Remote Sensing*, 2015, 53(4), 2021-2038. <https://doi.org/10.1109/TGRS.2014.2352555>
8. Di, M. G., Poderico, M., Poggi, G. Benchmarking Framework for SAR Despeckling. *IEEE Transactions on Geoscience and Remote Sensing*, 2014, 52(3), 1596-1615. <https://doi.org/10.1109/TGRS.2013.2252907>
9. Easley, G., Labate, D., Lim, W. Q. Sparse Directional Image Representation Using the Discrete Shearlets Transform. *Applied and Computational Harmonic Analysis*, 2008, 25(1), 25-46. <https://doi.org/10.1016/j.acha.2007.09.003>
10. Foucher, S., Lopez-Martinez C. Analysis, Evaluation, and Comparison of Polarimetric SAR Speckle Filtering Techniques. *IEEE Transactions on Image Processing*, 2014, 23(4):1751-1764. <https://doi.org/10.1109/TIP.2014.2307437>
11. Gabryel, M., Damaševičius, R. The Image Classification with Different Types of Image Features. In *Artificial Intelligence and Soft Computing*. Springer International Publishing, 2017, 497-506. [https://doi.org/10.1007/978-3-319-59063-9\\_44](https://doi.org/10.1007/978-3-319-59063-9_44)
12. Hu, S., Ma, X., Liu, S. SAR Image De-Noising Based on Non-local Similar Block Matching in NSST Domain. *IEEE International Conference on Signal Processing*, 2017, 832-836. <https://doi.org/10.1109/ICSP.2016.7877947>
13. Ke, Q., Zhang, J., Wei, W., Damasevicius, R., Wozniak, M. Adaptive Independent Subspace Analysis of Brain Magnetic Resonance Imaging Data. *IEEE Access*, 2019, 7, 12252-12261. <https://doi.org/10.1109/ACCESS.2019.2893496>
14. Kuan, D. T., Sawchuk, A. A., Strand, T. C. Adaptive Noise Smoothing Filter for Image with Signal-dependent Noise. *IEEE Transactions on Pattern Analysis and Machine Intelligence*, 1985, 7(2), 165-177. <https://doi.org/10.1109/TPAMI.1985.4767641>
15. Kutyniok, G., Labate, D. *Shearlets: Multiscale Analysis for Multivariate Data*. Birkhäuser Basel, 2012, 1-38. [https://doi.org/10.1007/978-0-8176-8316-0\\_1](https://doi.org/10.1007/978-0-8176-8316-0_1)
16. Lee, J. S. Digital Image Enhancement and Noise Filtering by Use of Local Statistics. *IEEE Transactions on Pattern Analysis and Machine Intelligence*, 1980, 2(2), 165-168. <https://doi.org/10.1109/TPAMI.1980.4766994>



17. Lim, W. Q. The discrete Shearlet Transform: a New Directional Transform and Compactly Supported Shearlet Frames. *IEEE Transactions on Image Processing*, 2010, 19(5), 1166-1180. <https://doi.org/10.1109/TIP.2010.2041410>
18. Liu, J., Qiu, X., Hong, W. Automated Ortho-rectified SAR Image of GF-3 Satellite Using Reverse-range-doppler Method. *International Geoscience and Remote Sensing Symposium*, Beijing, China, 2016, 4445-4448. <https://doi.org/10.1109/IGARSS.2016.7730158>
19. Liu, S., Liu, M., Li, P., Zhao, J., Zhu, Z., Wang, X. SAR Image Denoising Via Sparse Representation in Shearlet Domain Based on Continuous Cycle Spinning. *IEEE Transactions on Geoscience and Remote Sensing*, 2017, 55(5), 2985-2992. <https://doi.org/10.1109/TGRS.2017.2657602>
20. Parrilli, S., Poderico, M., Angelino, C. V., Verdoliva, L. A Nonlocal SAR Image Denoising Algorithm Based on LLMMSE Wavelet Shrinkage. *IEEE Transactions on Geoscience and Remote Sensing*, 2012, 50(2), 606-616. <https://doi.org/10.1109/TGRS.2011.2161586>
21. Qiang, Y., Zhang, J. A Bijection Between Lattice-Valued Filters and Lattice-Valued Congruences in Residuated Lattices. *Mathematical Problems in Engineering*, 2013, Article ID 908623. <https://doi.org/10.1155/2013/908623>
22. Rao, G., Peng, Y., Xu, Z. Robust Sparse and Low-rank Matrix Decomposition Based on Modeling. *Scientia Sinica Informationis*, 2013, 43(6), 733-748. DOI 10.1360/112012-538
23. Rezaei, H., Karami, A. SAR Image Denoising Using Homomorphic and Shearlet Transforms. *International Conference on Pattern Recognition and Image Analysis*, 2017, 80-83. <https://doi.org/10.1109/PRIA.2017.7983022>
24. Shao, W., Sheng, Y., Sun, J. Preliminary Assessment of Wind and Wave Retrieval from Chinese GF-3 SAR Imagery. *Sensors*, 2017, 17(8), 1-13. <https://doi.org/10.3390/s17081705>
25. Sharma, A., Bhateja, V., Tripathi, A. An Improved Kuan Algorithm for Despeckling of SAR Images Information Systems Design and Intelligent Applications. Springer India, 2016, 663-672. [https://doi.org/10.1007/978-81-322-2752-6\\_65](https://doi.org/10.1007/978-81-322-2752-6_65)
26. Sun, Z. Gamma-Distributed Maximum a Posteriori Despeckling Algorithm of High-Resolution Synthetic Aperture Radar Images. *Acta Physica Sinica*, 2013, 62(18), 81-86. DOI:10.7498/aps.62.180701
27. Sun, Z., Song, H., Wang, H., Fan, X. Energy Balance-Based Steerable Arguments Coverage Method in WSNs. *IEEE Access*, 2017, 99(6), 33766-33773. <https://doi.org/10.1109/ACCESS.2017.2682845>
28. Touzi, R. A Review of Speckle Filtering in the Context of Estimation Theory. *IEEE Transactions on Geoscience and Remote Sensing*, 2002, 40(11), 2392-2404. <https://doi.org/10.1109/TGRS.2002.803727>
29. Xie, H., Pierce, L. E., Ulaby, F. T. SAR Speckle Reduction Using Wavelet Denoising and Markov Random Field Modeling. *IEEE Transactions on Geoscience and Remote Sensing*, 2002, 40(10), 2196-2212. <https://doi.org/10.1109/TGRS.2002.802473>
30. Xu, Q., Wang, L., Hei, X. H., Shen, P., Shi, W., Shan, L. GI/Geom/1 Queue Based on Communication Model for Mesh Networks. *International Journal of Communication Systems*, 2014, 27(11), 3013-3029.
31. Xu, Z. B., Guo, H. L., Wang, Y., Zhang, H. Representative of Regularization Among  $(0 < q \leq 1)$  regularizations: An Experimental Study Based on Phase Diagram. *Acta Automatica Sinica*, 2012, 38(7), 1225-1228. [https://doi.org/10.1016/S1874-1029\(11\)60293-0](https://doi.org/10.1016/S1874-1029(11)60293-0)
32. Xu, Z., Wu, Y., Zhang, B. Sparse Radar Imaging Based on Regularization Theory. *Chinese Science Bulletin*, 2018, 63(14), 1307-1319+1306. <https://doi.org/10.1007/s11432-012-4632-5>
33. Yang, X. L., Zhou, B., Feng, J., Shen, P. Y. Combined Energy Minimization for Image Reconstruction from Few Views. *Mathematical Problems in Engineering*, 2012. <https://doi.org/10.1155/2012/154630>
34. Yi, Z. L., Yin, D., Hu, A. Z., Zhang, R. SAR Image Despeckling Based on Non-local Means Filter. *Journal of Electronics and Information Technology*, 2012, 34(4), 950-955. DOI:10.3724/SP.J.1146.2011.00918
35. Yommy, A. S., Liu, R., Onuh, S. O., Ikechukwu, A. C. SAR Image Despeckling and Compression Using K-nearest Neighbour Based Lee Filter and Wavelet. *International Congress on Image and Signal Processing*, IEEE, 2016, 158-167. <https://doi.org/10.1109/CISP.2015.7407868>
36. Zhang, Q. System Design and Key Technologies of the GF-3 Satellite. *Acta Geodaetica et Cartographica Sinica*, 2017, 46(3), 269-277. DOI: 10.11947/j. AGCS.2017.20170049
37. Zheng, Y., Xu, M., Wang, L. Improved Weighted Non-local Means Ultrasonic Image Denoising Algorithm. *Journal of Image and Graphics*, 2017, 22(6), 778-786.

